

Full Paper

Electrochemical Desorption of Proteins from Gold Electrode Surface

Shankar Balasubramanian,^a Alexander Revzin,^{b*} Aleksandr Simonian^{a*}

^a Materials Research and Education Center, Auburn University, Auburn AL 36849

*e-mail: als@auburn.edu

^b Department of Biomedical Engineering, University of California, Davis CA 95616

*e-mail: arevzin@ucdavis.edu

Received: July 10, 2006

Accepted: July 27, 2006

Abstract

The goal of this study was to enable rational modulation of biological interfaces using electrochemical desorption of surface-bound proteins. Coupled, surface plasmon resonance (SPR) – electrochemistry instrument was used to monitor molecular assembly events on gold electrodes and to correlate these events with changes in electrochemical properties of the substrate. Model proteins, bovine serum albumin (BSA) and immunoglobulin G (IgG), were conjugated via carbodiimide (EDC) chemistry to a layer of mercaptoundecanoic acid (MUA) assembled on SPR sensor surface. Deposition of alkanethiols and proteins were monitored by ellipsometry and SPR techniques, and was further confirmed by cyclic voltammetry with potassium ferricyanide serving as a reporter molecule. The surface-bound proteins were completely removed by applying a reductive potential of -1200 mV vs. Pt electrode in a physiological saline buffer. Importantly, the sequence of protein immobilization followed by desorption could be repeated multiple times, thus demonstrating ability to modulate interfacial properties. Controlled removal of protein molecules from electrode surfaces is envisioned to have important applications in affinity or cell-based biosensing, cellular micropatterning and cell sorting.

Keywords: Electrochemical desorption, Alkanethiols, Surface-bound proteins, Controlled removal, Surface plasmon resonance, Electrochemistry

DOI: 10.1002/elan.200603627

1. Introduction

Precise design of biointerfacial properties is emerging as a key factor in the fields of biosensing and cellular engineering. Gold is commonly used for fabrication of working electrodes; therefore, defining surface properties of this material is important for electrochemical sensor development and electrical manipulation of cells. Modifying gold surfaces by self-assembly of alkanethiols has been the subject of intense investigation over the past twenty years [1–4]. By synthesizing appropriate alkanethiol molecules, gold surfaces can be rendered nonfouling, through the inclusion of poly(ethylene glycol) molecules, or protein-reactive, by incorporating aliphatic or reactive polar groups [3, 4]. In addition, there is interest in controlling surface properties in a spatial and/or temporal fashion [2, 5–10]. Regional control of surface properties can be exercised by designing substrates composed of different materials and then using self-assembling molecules specific to these materials (e.g., thiols/silane for gold/silicon [9], electrical wiring of proteins by reconstitution of cofactor modified monolayers assembled onto Au-electrodes [11], or thiols/carboxylic acids for gold/ Al_2O_3 [2]). Another approach to controlling spatiotemporal properties of gold electrode surfaces is exemplified by works of Lahann [10] and Mrksich

[8] whereby self-assembled monolayer undergoes conformational or compositional changes when electrical potential is applied, thus, resulting in switching of surface properties. The third approach is based on the ability to strip self-assembled alkanethiols from gold via electrochemical reduction [12]. This method has been used to create molecular and protein concentration gradients on gold [5, 6] as well as design cell motility assays [7]. While the reports of alkanethiol desorption from gold are common [12–15], studies pertaining to electrochemical removal of large protein molecules covalently immobilized to self-assembled alkanethiols are infrequent.

Therefore, the main goal of the present study was to determine feasibility of removal of model proteins covalently bound to gold electrode surfaces. In order to observe molecular binding events in real-time and to correlate these events to changes in electrical properties of the gold surface, we employed combined electrochemical-surface plasmon resonance (ESPR) instrument described in our prior work [16]. Additional surface characterization was carried out by ellipsometry. Model proteins, bovine serum albumin (BSA) and immunoglobulin G (IgG) were covalently bound to self-assembled mercaptoundecanoic acid (MUA) through carbodiimide (EDC/NHS) chemistry. Deposition of alkanethiols and proteins was monitored by SPR and confirmed by

cyclic voltammetry with potassium ferricyanide serving as a probe molecule. Estimation of the surface coverage based on SPR signals showed formation of densely packed alkanethiol and protein layers. Significantly, electrochemistry and SPR experiments showed that these layers were completely removed from gold surface after applying a reductive potential (-1.2 V vs. Pt electrode). The sequence of alkanethiol/protein assembly steps followed by electrochemical stripping could be repeated multiple times, demonstrating the ability to modulate gold electrode properties. Studies described here are envisioned to have significant applications in the areas of affinity or cell-based biosensing, as well as, in developing tools for micropatterning and sorting of living cells.

2. Experimental

2.1. Chemicals

O-[2-(3-Mercaptopropionylamino) ethyl]-*O'*-methylpolyethylene glycol (PEG-thiol), 11-mercaptopundecanoic acid (MUA), 1-ethyl-3-(3-dimethylaminopropyl) carbodiimide (EDC), Phosphate buffered saline (PBS), and absolute ethanol were obtained from Sigma-Aldrich. Bovine serum albumin (BSA), Tris (hydroxymethyl) aminomethane, potassium hydroxide and ethanolamine were purchased from Fisher Scientific. *N*-hydroxysuccinimide (NHS) and Potassium ferricyanide, $K_3Fe(CN)_6$ (FCN) were obtained from Acros-Organics (through fisher). All the chemicals were used without further purification. Organophosphorous Hydrolase (OPH) enzyme and anti-OPH were obtained from Texas A&M University and was used as is.

2.2. Surface Preparation and Characterization

Sensing surfaces were cleaned using piranha solution (3:1: H_2SO_4 and H_2O_2 . **Caution:** Piranha solution is dangerous and should be handled with care) for 5 minutes and rinsed thoroughly with deionized (DI) water. The efficacy of cleaning of the sensor surface was confirmed by validating the refractive index (RI) of water as 1.333. Prior to SPR experiments, the sensor surface was made hydrophilic by air-plasma cleaning for 5 minutes (Harrick Scientific). After plasma cleaning, the sensor was docked with the ESPR cell and references were obtained in air and water. For ellipsometry and atomic force microscopy measurements, glass slides were coated with ca. 2 nm chromium adhesion layer followed by ca. 50 nm gold film and were cleaned with piranha solution as described above. These surfaces were then sonicated in acetone for 5 min., rinsed with DI water, and then sonicated with ethanol for 5 min. After sonication, gold coated glass slides were plasma cleaned in air for 5 minutes and immediately immersed in 1 mM ethanolic solution of MUA for ca. 18 to 20 h. The slides were then rinsed with ethanol and water and modified with proteins as in Section 2.4.

Ellipsometric measurements were carried out using a commercially available ellipsometer (Auto ELLE3, Rudolph Research, Inc). The thickness of immobilized multilayer was determined by null ellipsometry with refractive indices taken to be 1.45 for alkanethiols and proteins [17, 18].

2.3. Combined Electrochemical-SPR Measurement

For combined electrochemical-SPR studies, SPREETA sensors developed by Texas Instrument (TI) were used. This SPR system employs a light emitting diode (840 nm) with a polarizer, reflecting mirror, and Si-photodiode array. The sensing region is coated with a semitransparent gold film (ca. 50 nm) with a Cr-adhesion layer (1–2 nm). A 12-bit three-channel electronic control box completes the interface between the sensor and a PC. Multichannel SPREETA software provided by TI monitors the changes in RI near the sensing surface, calculates the statistical noise in the signal and displays the results. The signal is generally displayed in the response unit (RU) (1 Response Unit = 10^{-6} Refractive index unit), and the Spreeta sensor's detection limit is ca. 10^{-6} refractive index units. All the SPR experiments were carried out in batch mode with no flow setup. A custom built electrochemical-SPR cell (ESPR cell) was made of Teflon with openings for inserting both reference electrode (Ag/AgCl, BAS) and platinum counter electrode (Pt foil). Two types of electrochemistry experiments were carried out. Electrochemical reduction experiments were performed in situ in a two or three electrode set-up with SPR sensor gold surface serving as a working electrode (Fig. 1). BAS CV-

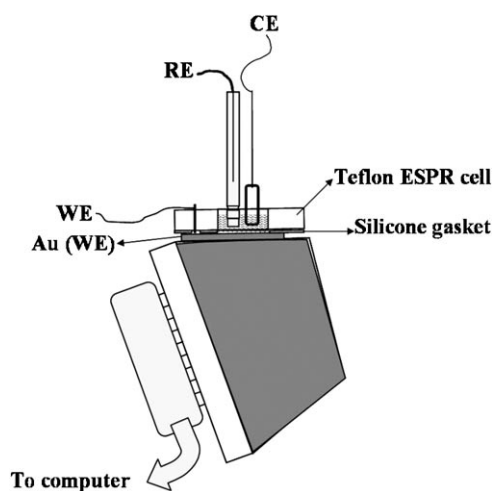


Fig. 1. Combined electrochemical SPR (ESPR) setup. A home-made electrochemical-SPR cell (ESPR cell) was used for all ESPR experiments. SPREETA sensor containing gold electrode was used as working electrode (WE), while Ag/AgCl and Pt foil were used as reference electrode and auxiliary electrode respectively. For two-electrode process, the Ag/AgCl reference electrode (RE) was removed and potential was applied against Pt counter electrode (CE). The RE and CE leads from the potentiostat were both connected to the Pt electrode in order to use potentiostat as power source.

50W potentiostat was used to apply reductive potential. In a second type of electrochemistry experiment, cyclic voltammetric measurements were used to characterize presence of passivating (resistive) layers on the electrode surface. In these experiments, three electrode system consisting of gold working electrode (BAS, $\varnothing = 1.6$ mm), Pt foil as counter electrode and Ag/AgCl reference electrode were employed. Initially, the gold electrode was mechanically polished using alumina and rinsed thoroughly with water. Remaining alumina particles were removed by sonication in water for ca. 3 minutes.

2.4. Adsorption and Desorption of Proteins from SPR Sensor Surface

Prior to assembly of molecular components, SPR sensor surface was washed with 0.12 M NaOH and 1% Triton X solution. After this washing step, a baseline was obtained in fresh PBS buffer. Clean gold surfaces were modified with self-assembled monolayer (SAM) of 1 mM MUA in ethanol for 75 minutes followed by thorough rinsing with ethanol and DI water. Proteins were immobilized on the SAM by activating the carboxylic acid groups of 11-MUA with freshly prepared 0.4 M EDC/0.1 M NHS in water for 15 minutes. The activated surface was reacted with BSA (1 mg/mL) in PBS (10 mM, pH 7.4) to covalently bind this protein to MUA-covered gold surface. After conjugation of BSA for ca. 75 minutes, the surface was rinsed with PBS buffer to remove unreacted protein molecules. Antibody immobilization occurred by a similar protocol, where 0.1 mg/mL anti-OPH antibody was reacted with activated MUA monolayer for ca. 1 h and washed with PBS buffer. 50 mM Tris buffer was used to quench the activated carboxyl groups of MUA to eliminate further chemical reaction with free amines. A low concentration of antigen OPH (35 nM) was introduced and subsequently captured by the immobilized antibody. Unbound OPH molecules were washed away with buffer solution.

Reductive desorption of immobilized molecules were carried out using two-electrode system. A reductive potential of -1200 mV was applied against Pt counter electrode for 30 seconds and the surface was immediately washed with PBS to avoid re-adsorption of alkanethiol molecules.

The thickness and surface coverage of individual adlayers were calculated assuming 'linear response regime' of the evanescent wave, in which the thickness of the adlayers is $d_a < l_d$, (l_d is the decay length of the evanescent wave) [19]. Given that the thickness of most of the SAMs and proteins are on the order of few nanometers whereas the decay length of the evanescent wave is on the order of 200 nm [13], this relationship should hold true. Thickness of the adsorbed layer was calculated using Equation 1 shown below:

$$d_a = (l_d/2) (n_{\text{eff}} - n_b)/(n_a - n_b) \quad (1)$$

where d_a is the thickness of the layer, l_d is the characteristic decay length, n_{eff} is the effective refractive index measured

by SPR, n_b is the refractive index of buffer obtained from the buffer baseline before individual assembly step, and n_a is the refractive index of adlayer. For proteins and alkanethiols n_a was taken to be 1.45. Once the thickness is known, the surface coverage (in g/mm^2 or mole/mm^2) may be derived from the bulk density of the molecule. Bulk density values for proteins and MUA were taken to be $1.3 \text{ g}/\text{cm}^3$ [19] and $0.792 \text{ g}/\text{cm}^3$ (from www.sigma-aldrich.com), respectively.

3. Results and Discussions

The present study employed coupled electrochemistry-SPR instrument to demonstrate electrochemical removal of proteins covalent bound to the gold electrode surface. Ability to exercise dynamic control over molecular assembly events demonstrated here has important applications in the fields of biosensing and cellular engineering.

3.1. Formation of SAM on Gold

Ellipsometry, SPR and electrochemistry were used in concert throughout this study to verify assembly and removal of molecules from electrode surfaces. Figure 2 shows, diagrammatically, step-by-step procedure used in this study to immobilize model proteins on Au surfaces. Ellipsometry (Fig. 3) was performed to confirm assembly of multiple layers on Au electrode surface. MUA thickness measured by ellipsometry was ca. 2 nm which points to formation of a monolayer and is in good agreement with the values of 1.9 nm reported in the literature [20, 21]. The observed thickness is also in good agreement with values expected for densely packed chains extending away from the surface [1, 22]. By converting SPR signal into thickness (see Section 2.4 for description of the method) the MUA layer was also determined to be ca. 1.9 nm, confirming our ellipsometry results. The surface coverage was determined from SPR signal to be $(7.04 \pm 0.01) \times 10^{-10} \text{ mol}/\text{cm}^2$. This value compares well with literature values of $7.6 \times 10^{-10} \text{ mol}/\text{cm}^2$ and, once again, indicates formation of a tightly packed alkanethiol monolayer [23, 24].

3.2. Immobilization of Proteins on Sensing Surfaces

Immobilization of proteins was carried out by activating carboxylic acid groups of MUA monolayer with EDC-NHS mixture. Proteins containing amine groups on the surface interact readily with the activated MUA intermediates and form covalent amide linkages. SPR was used to monitor covalent immobilization of proteins in real time. The thickness of protein layer was calculated according to the Equation 1 and compared to ellipsometry results. Figure 4a shows the real-time binding of BSA to EDC/NHS activated MUA layer. A sharp increase in RI was noticed for EDC/NHS injection, which is due to bulk refractive index change between buffer and EDC/NHS in water. After rinsing with

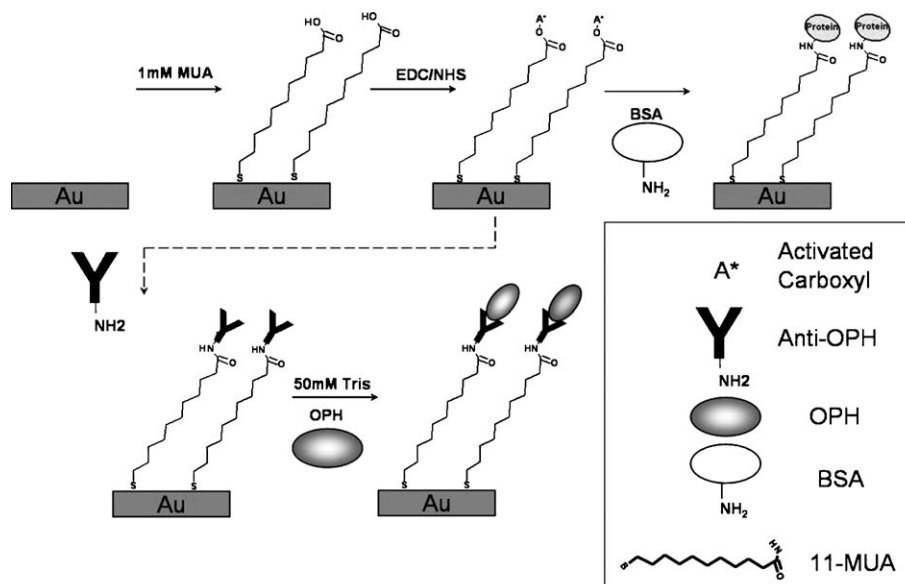


Fig. 2. Schematic of a sequence of surface modification steps employed in the study.

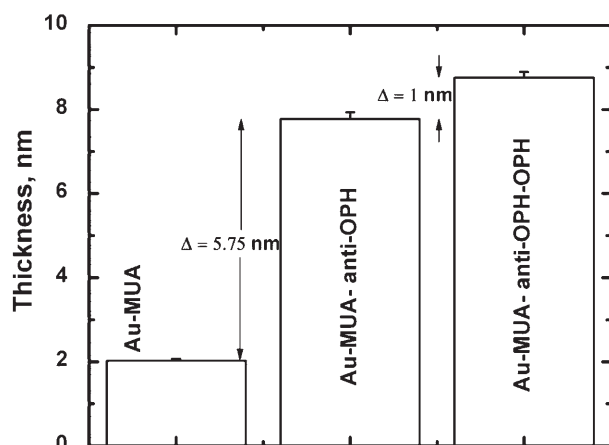


Fig. 3. Ellipsometric thickness measurements for gold surface modified with anti-OPH immobilized on MUA SAM.

buffer, BSA of 1 mg/mL solution was reacted with the surface for ca. 75 minutes. The surface was then washed with buffer to remove nonspecifically or loosely adsorbed molecules. Since, at pH 7.4 BSA carries a net negative charge, nonspecific adsorption of BSA to MUA ($pK_a \approx 6.5$

[25]) under neutral pH is not expected to be significant. SPR signal associated with BSA binding (shown in Figure 4), corresponded to surface coverage of $(1.08 \pm 0.14) \text{ ng/mm}^2$ or $(9.68 \pm 1.2) \times 10^{11} \text{ molecules/cm}^2$. Similar coverage values (1.2 to 1.8 ng/mm^2) were reported in the literature [19, 26]. To determine approximate ideal surface coverage for a given protein, a simple approximation has been shown to work [27]:

$$P_{\text{ideal}} \approx MW/\pi ab N_a \quad (2)$$

where, P is surface coverage, MW is molecular weight of the protein, a and b are dimensions of the molecule and N_a is Avagadro's number. Using this relationship and assuming BSA to be a spherical molecule with approximate dimensions of $5 \times 5 \times 5 \text{ nm}$ [28], P_{ideal} was calculated to be 1.4 ng/mm^2 . This translates to ca. 77% surface coverage for BSA molecules.

In addition to BSA, we investigated surface deposition and removal of an antibody specific to organophosphorous hydrolase (OPH) – an enzyme hydrolyzing organophosphate neurotoxins. Anti-OPH antibody was reacted for 1 h with Au surfaces containing EDC/NHS activated MUA layer. Binding of antibody resulted in a SPR signal of ca.

Table 1. Adlayer thickness from SPR measurements.

Adlayer	Adlayer thickness (nm, SPR)	Surface coverage (molecules/cm ²)	Adlayer thickness (nm, ellipsometry)
MUA	1.9 ± 0.18	$4.15(\pm 0.4) \times 10^{14}$	2.02 ± 0.05
BSA	0.83 ± 0.1	$9.68(\pm 1.2) \times 10^{11}$	–
MUA	1.98 ± 0.13	$4.33 (\pm 0.29) \times 10^{14}$	2.05 ± 0.08
Anti-OPH	1.86 ± 0.45	$9.69 (\pm 2.3) \times 10^{11}$	5.75 ± 0.2
OPH	1.48 ± 0.05	$1.61(\pm 0.05) \times 10^{12}$	1 ± 0.02

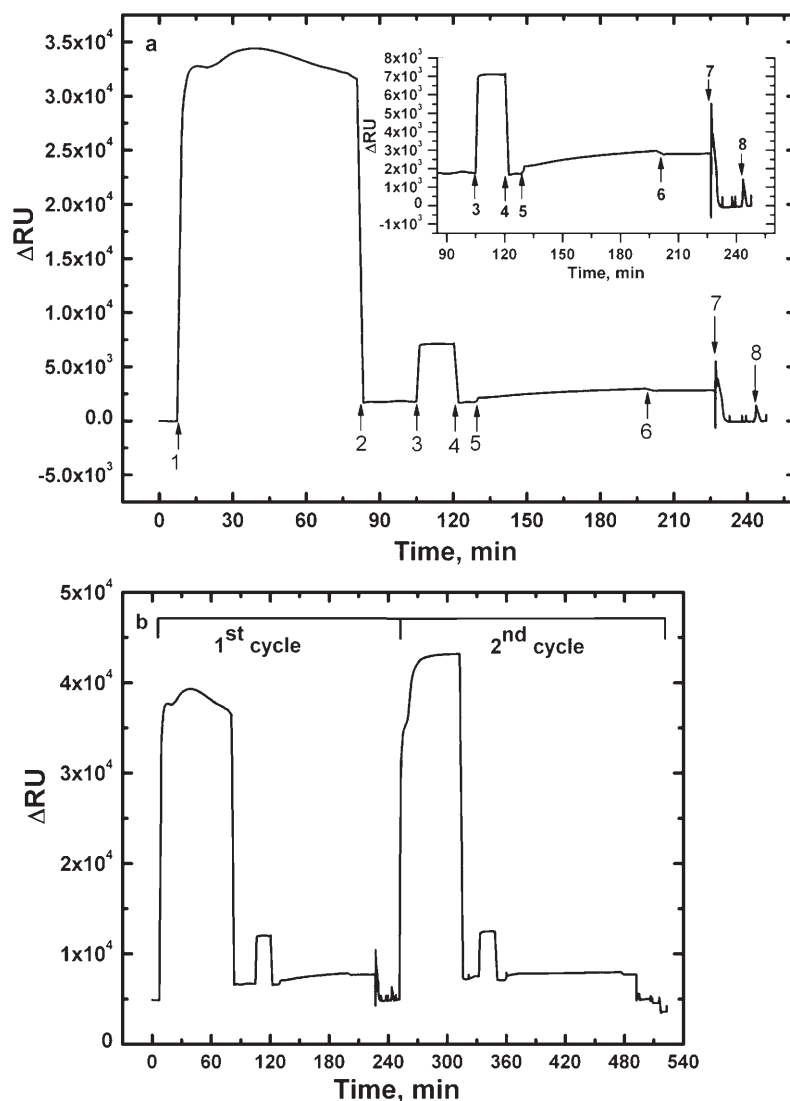


Fig. 4. a) Protein immobilization and reductive desorption using SPR. The sequences of the steps are as follows: 1) modification with 1 mM MUA; 2) washing with ethanol and PBS; 3) activation of surface carboxylates using 0.4 M EDC/0.1 M NHS mixture; 4) washing with PBS; 5) covalent immobilization of BSA (1mg/mL) to the activated SAM surface; 6) PBS wash and; 7) reductive desorption of the immobilized molecules at -1200 mV vs. Pt electrode in PBS using two-electrode setup and 8) confirmation of reductive desorption by applying -1200 mV. Insert figure shows the steps 3 to 8. b) Two cycles demonstrating adsorption and desorption of BSA from the electrode surface. These results point to possibility of regenerating electrode surface.

1500 Δ RU (see Fig. 5) compared to ca. 1000 Δ RU for BSA. This difference in signal is expected given the larger size of an IgG molecule (150 kDa) compared with BSA (66 kDa). After antibody immobilization, unconjugated active carboxyl groups of MUA were quenched with Tris buffer (50 mM) followed by PBS washing. Binding of the antibody resulted in a significant SPR signal (ca. 600 Δ RU). Injection of OPH (35 nM) followed by buffer washing produced an additional signal of ca. 500 Δ RU (see inset of Figure 5). SPR signal from antibody binding was converted to surface coverage in a fashion similar to that described for BSA. The surface coverage for antibody was found to be $9.69 (\pm 2.3) \times 10^{11}$ molecules/cm² or 1.67 ng/mm² whereas OPH had $1.61 (\pm 0.05) \times 10^{12}$ molecules/cm². Therefore, each antibody molecule was bound to roughly 1.6 OPH molecules, which is

expected given that this bivalent antibody captures two antigen molecules. These results offer a direct proof that covalently bound antibody retained activity and ability to bind its antigen.

Using Equation 2, taking dimensions of the antibody to be 14.5×8.5 nm [29], and assuming ellipsoidal projection onto a plane, P_{ideal} for IgG protein (MW 150 000 Da) is approximated to be 0.64 ng/mm². Given the actual surface density of 1.67 ng/mm² determined by SPR measurements and Equation 1, the surface coverage for IgG is ca. 260%, pointing to some possibility of multilayer formation. This value may not be precise as it hinges on the approximate relationship described in Equation 2 and assumes that antibody molecule creates an elliptical projection onto an xy plane. However, our surface coverage estimations do

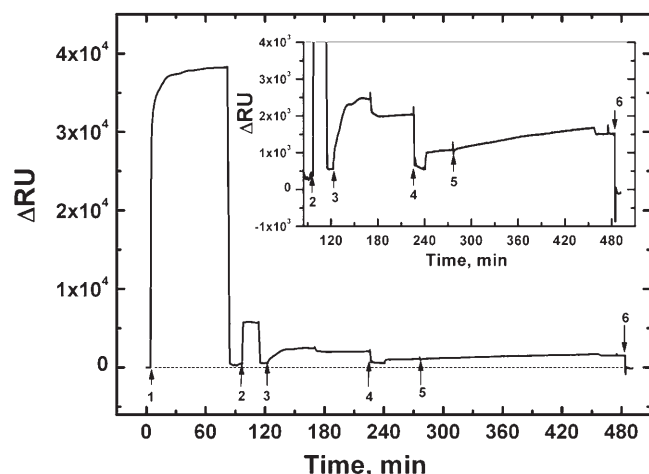


Fig. 5. Anti-OPH antibody immobilization and reductive desorption using SPR. The sequences of the steps are follows: 1) modification with 1 mM MUA, 2) activation of surface carboxylates using 0.4 M EDC/0.1 M NHS mixture, 3) covalent immobilization of anti-OPH (0.1 mg/mL) to the activated SAM surface, 4) quenching with 50 mM Tris buffer, 5) injection of OPH (35 nM), and 6) Reductive desorption of the immobilized molecules at -1200 mV vs. Pt electrode in PBS using two-electrode setup. Insert figure represents the steps from 2 to 6.

point to formation of dense layers of IgG and BSA molecules on the gold electrode surface.

3.3. Reductive Desorption of Immobilized Proteins Through SAM

Preceding sections of this article ascertained formation of a densely packed alkanethiol and protein layers on gold. Question central to this study was whether proteins could be removed by reductive desorption of the underlying alkanethiol monolayer? Electrochemical-SPR (ESPR) instrument is a perfect tool for probing such questions. This instrument allows to monitor molecular assembly events in real-time, to apply electrical potential in situ and then to observe subsequent changes in the composition of the biointerface. Prior to performing protein-stripping experiments, ability to perform electrochemistry on the SPR sensor surface was demonstrated. Figure 6a shows a representative cyclic voltammetry experiment performed in HClO_4 solution using SPR sensor surface as working electrode. The shape of the curve is similar to results reported previously for Au (111) in HClO_4 solution [30–32]. The region from 0.2 to 0.92 V corresponds to the double layer charging effect while the oxidation of gold electrode commences at 0.96 V. The two peaks denoted as OA I (1.1 V) and OA II (1.19 V) have previously been attributed to two-electron transfer involved in the oxidation of gold to gold oxide [30, 31]. There is also dependence of the SPR curve on the applied potential as shown in Figure 6b. The peaks OA I and OA II can be observed in the ΔRI vs. potential curve while the sharp reduction in the current vs.

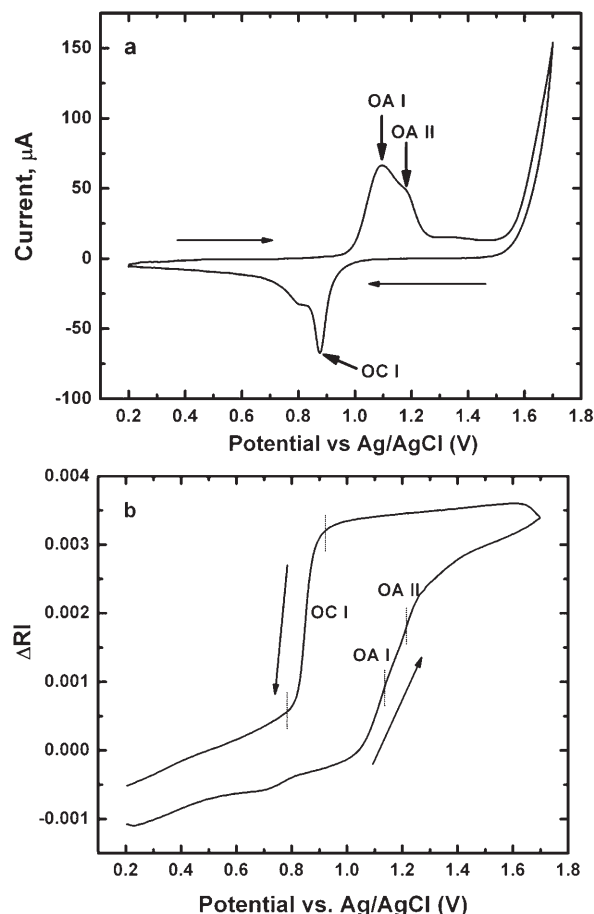


Fig. 6. Cyclic voltammogram of 0.1 M HClO_4 from combined ESPR setup. a) Cyclic voltammogram collected using ESPR device; b) ΔRI vs. E , i.e., potential-dependent change in SPR response.

potential curve (Fig. 6a) is seen as sudden drop in ΔRI occurring around 0.89 V. These changes in SPR response for interfacial process on the bare electrode have been reported in the literature [33, 34]. It is important to note that the SPR signal is only affected by the electrical field while the potential is being applied. It stabilizes once the electrochemical experiment is stopped. Effects of applied potential on the SPR readout are manifested by sharp drops in ΔRI signal seen for example in step 7 of Figure 4, where reductive potential is applied. However, as one can see from this Figure, SPR signal stabilizes afterwards.

After validating ESPR instrument, electrochemistry experiments were performed in situ using SPR sensor as a working electrode. These experiments were used to complement SPR sensograms. Figure 5 shows SPR sensogram of assembly of anti-OPH antibody on activated alkanethiol monolayers. Results shown in this Figure can be correlated with Figure 7 where surface properties of the SPR sensor are characterized by cyclic voltammetry (CV) with potassium ferricyanide as redox species. As seen from Figure 7, assembly of MUA followed by the antibody immobilization passivates the electrode surface, prevents electron exchange between the redox molecule and the electrode, and almost

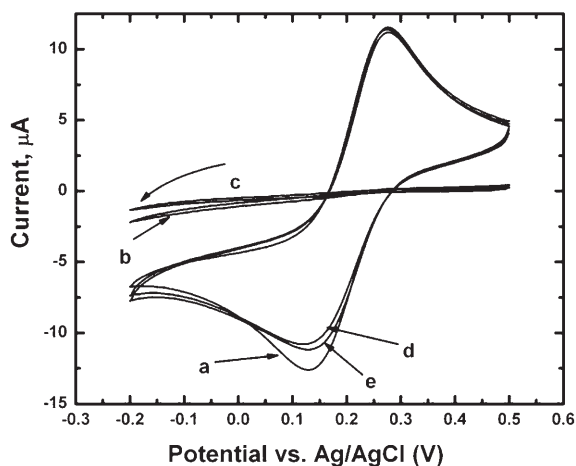


Fig. 7. Cyclic voltammogram of commercial BAS electrode modified with SAM and antibody. All the CV's were performed in 5mM FCN solution prepared in 10 mM PBS, pH 7.4. a) Bare gold electrode; b) gold electrode modified with 1mM MUA for 20 h; c) gold electrode modified with antibody (1 h) after SAM activation with EDC/NHS mixture; d) after reductive desorption using two-electrode system at -1200 mV vs. Pt electrode; and e) after reductive desorption using two-electrode system at -1400 mV vs. Pt electrode.

completely eliminates anodic/cathodic redox peaks of potassium ferricyanide. Time-based amperometry was used to remove this resistive molecular layer and to regenerate the electrode surface. Previous studies reported that reductive desorption of alkanethiols from Au occurred at -0.9 V [14, 35] vs. Ag/AgCl reference electrode. To ensure that both the alkanethiol and protein layers are removed, the gold electrode was biased at -1.2 V (vs. Pt electrode) for 30 s in PBS buffer. Desorption of MUA and antibody layers was verified by CV with ferricyanide. Figure 7d demonstrates regeneration of the electrode surface and appearance of ferricyanide redox peaks similar in magnitude to an unmodified electrode. Additional desorption experiment carried out at -1.4 V for 30 s in PBS only slightly improved the shape of the ferricyanide CV as shown in Figure 7e.

Combined ESPR experiment using BSA confirm the above results (see Fig. 4). After covalent immobilization of BSA to chemisorbed SAMs, the SPR gold electrode was polarized at -1.2 V vs. Pt electrode. After reductive electrochemical desorption, SPR response returns to its initial baseline, demonstrating the complete removal of BSA/MUA layers (see Fig. 4a, step 7). A second application of -1.2 V did not significantly change the SPR response (Fig. 4a, step 8). Assembly and removal of protein molecules coupled to alkanethiols is repeatable, as demonstrated by Figure 4b which shows two cycles of BSA/MUA adsorption and desorption. Thus, the electrochemical desorption enables regeneration of the electrode surface for further use modification.

Similar desorption experiments were performed to remove antigen–antibody couple from the electrode surface. Figure 5 shows representative ESPR curve for these experi-

ments. After immobilizing the anti-OPH antibody through EDC/NHS chemistry, antigen (OPH) was introduced to interact with anti-OPH. Antibody–antigen pair was removed from the surface by electrochemical desorption of underlying alkanethiol by applying reductive potential of -1.2 V vs. Pt electrode in PBS. As seen in the Figure 5 (insert, step 6) SPR signal drops sharply after reductive desorption and reaches its starting baseline (Fig. 5, main, step 6). Results presented in Figure 5 demonstrate that active antibodies can be immobilized on the electrode surfaces and subsequently removed by applying reductive potential. These results are important as a demonstration of electrode surface regeneration. In addition, removal of biomolecules from the electrode surface may be coupled with a fluidic delivery and down stream sample analysis in the future.

4. Conclusions

While electrochemical stripping of alkanethiols has been reported widely as a method of biointerface engineering, removal of large protein molecules covalently bound to alkanethiols has not been demonstrated. This study employed electrochemistry and SPR techniques to assemble model proteins, BSA and IgG, on alkanethiol-modified gold electrode surfaces. SPR characterization of the molecular assembly pointed to formation of a densely packed MUA layer followed by covalent attachment of model proteins. Surface coverage for BSA and IgG was estimated being 77% and 260% respectively, pointing to the abundance of protein molecules present on gold. Complete removal of proteins through reductive desorption of underlying MUA was verified by electrochemical-SPR instrument and by cyclic voltammetry performed in parallel. Controlled desorption of proteins from the gold surface demonstrated in this study represents simple and effective method for designing electrode surface properties. Approach presented here will be applicable in biosensor development, where it may be used to assemble different sensing elements onto individually addressable gold microelectrodes. Controlling protein deposition and removal also defines the surface as cell-adhesive or nonadhesive. Therefore, electrochemistry methods presented here may be used to pattern multiple cells on the surface or to remove cells that are interacting with surface-bound proteins.

5. Acknowledgements

Support for this work comes from Auburn University Detection and Food Safety Center, from NSF Grant (CTS-0330189 to ALS) and from UC Davis start-up funds (AR). We are grateful to Prof. J. Wild (Texas A&M University) for providing OPH and anti-OPH antibody. Authors would like to acknowledge Adam Anderson and Anand Sankarraj for their help in ellipsometry and electrochemical experiments.

6. References

- [1] C. D. Bain, E. B. Troughton, Y. T. Tao, J. Evall, G. M. Whitesides, R. G. Nuzzo, *J. Am. Chem. Soc.* **1989**, *111*, 321.
- [2] P. E. Laibinis, J. J. Hickman, M. S. Wrighton, G. M. Whitesides, *Science* **1989**, *245*, 845.
- [3] J. C. Love, L. A. Estroff, J. K. Kriebel, R. G. Nuzzo, G. M. Whitesides, *Chem. Rev.* **2005**, *105*, 1103.
- [4] K. Prime, G. M. Whitesides, *Science* **1991**, *252*, 1164.
- [5] S. T. Plummer, Q. Wang, P. W. Bohn, R. Stockton, M. A. Schwartz, *Langmuir* **2003**, *19*, 7528.
- [6] R. H. Terrill, K. M. Balsas, Y. Zhang, P. W. Bohn, *J. Am. Chem. Soc.* **2000**, *122*, 988.
- [7] X. Y. Jiang, R. Ferrigno, M. Mrksich, G. M. Whitesides, *J. Am. Chem. Soc.* **2003**, *125*, 2366.
- [8] M. N. Yousaf, B. T. Houseman, M. Mrksich, *Proc. Natl. Acad. Sci.* **2001**, *98*, 5992.
- [9] S. Lan, M. Veiseh, Y. Zhang, *Biosens. Bioelectron.* **2005**, *20*, 1697.
- [10] J. Lahann, S. Mitragotri, T. N. Tran, H. Kaido, J. Sundaram, I. S. Choi, S. Hoffer, G. A. Somorjai, R. Langer, *Science* **2003**, *299*, 371.
- [11] I. Willner, V. HelegShabtai, R. Blonder, E. Katz, G. L. Tao, *J. Am. Chem. Soc.* **1996**, *118*, 10321.
- [12] V. M. Mirsky, *Trends Anal. Chem.* **2002**, *21*, 439.
- [13] A. Badia, S. Arnold, V. Scheumann, M. Zizlsperger, J. Mack, G. Jung, W. Knoll, *Sens. Actuators B* **1999**, *54*, 145.
- [14] S. Imabayashi, D. Hobarra, T. Kakiuchi, W. Knoll, *Langmuir* **1997**, *13*, 4502.
- [15] T. Kakiuchi, H. Usui, D. Hobarra, M. Yamamoto, *Langmuir* **2002**, *18*, 5231.
- [16] A. L. Simonian, A. Revzin, J. R. Wild, J. Elkind, M. V. Pishko, *Anal. Chim. Acta.* **2002**, *466*, 201.
- [17] B. L. Frey, C. E. Jordan, S. Kornguth, R. M. Corn, *Anal. Chem.* **1995**, *67*, 4452.
- [18] J. Voros, *Biophys. J.* **2004**, *87*, 553.
- [19] L. S. Jung, C. T. Campbell, T. M. Chinowsky, M. N. Mar, S. S. Yee, *Langmuir* **1998**, *14*, 5636.
- [20] C. E. D. Chidsey, D. N. Loiacono, *Langmuir* **1990**, *6*, 682.
- [21] E. L. Smith, C. A. Alves, J. W. Anderegg, M. D. Porter, L. M. Siperko, *Langmuir* **1992**, *8*, 2707.
- [22] M. D. Porter, T. B. Bright, D. L. Allara, C. E. D. Chidsey, *J. Am. Chem. Soc.* **1987**, *109*, 3559.
- [23] C. A. Widrig, C. A. Alves, M. D. Porter, *J. Am. Chem. Soc.* **1991**, *113*, 2805.
- [24] C. A. Widrig, C. Chung, M. D. Porter, *J. Electroanal. Chem.* **1991**, *310*, 335.
- [25] C. E. Jordan, R. M. Corn, *Anal. Chem.* **1997**, *69*, 1449.
- [26] V. Silin, H. Weetall, D. J. Vanderah, *J. Colloid Interface Sci.* **1997**, *185*, 94.
- [27] J. Lahiri, L. Isaacs, B. Grzybowski, J. D. Carbeck, G. M. Whitesides, *Langmuir* **1999**, *15*, 7186.
- [28] D. C. Carter, J. X. Ho, *Adv. Protein Chem.* **1994**, *45*, 153.
- [29] E. W. Silvertown, M. A. Navia, D. R. Davies, *Proc. Natl. Acad. Sci.* **1977**, *74*, 5140.
- [30] H. Angerstein-Kozłowska, B. E. Conway, A. Hamelin, L. Stoicoviciu, *Electrochim. Acta*, **1986**, *31*, 1051.
- [31] H. Angerstein-Kozłowska, B. E. Conway, A. Hamelin, L. Stoicoviciu, *J. Electroanal. Chem.* **1987**, *228*, 429.
- [32] S. Ye, C. Ishibashi, K. Shimazu, K. Uosaki, *J. Electrochem. Soc.* **1998**, *145*, 1614.
- [33] Y. Iwasaki, T. Horiuchi, M. Morita, O. Niwa, *Electroanalysis*, **1997**, *9*, 1239.
- [34] M. Tian, W. G. Pell, B. E. Conway, *J. Electroanal. Chem.* **2003**, *552*, 279.
- [35] M. R. Anderson, R. Baltzersen, *J. Colloid Interface Sci.* **2003**, *263*, 516.